

Resonant transmission in a dielectric photonic crystal with a thin metallic coating

TZU-CHYANG KING, PEI-CHIU TSAI, YA-LING LIN, CHI-CHUNG LIU^a, CHIEN-JANG WU^{b,*}

Department of Applied Physics, National Pingtung University of Education, Pingtung 900, Taiwan

^a*Department of Electro-Optics Engineering, National Formosa University, Yunlin 632, Taiwan*

^b*Institute of Electro-Optical Science and Technology, National Taiwan Normal University, Taipei 116, Taiwan*

In this work, the resonant optical transmission (ROT) in a dielectric-dielectric photonic crystal (DDPC) with a thin metallic coating operating in the visible is theoretically investigated. First, the phenomenon of ROT is shown to occur at the frequency within the photonic band gap (PBG). To obtain a significant ROT, there is an optimum stack number for the DDPC and an optimum thickness of thin metal layer. The phenomenon of ROT can be explained by the condition of impedance matching. Second, the effect of different metallic films on the ROT is also examined. It is found that the frequency of ROT is blue-shifted for the metal with a larger plasma frequency. Finally, the behavior of ROT is investigated as a function of angle of incidence for both TE and TM waves. The frequency of ROT is blue-shifted as the angle of incidence increases for TE and TM waves. In TM wave, it is of interest to find that there are two ROTs within the photonic band gaps. The analysis made is based on the use of the transfer matrix method.

(Received October 19, 2012; accepted September 18, 2013)

Keywords: Photonic crystal, Resonant transmission, Photonic band gap

1. Introduction

Engineering photonic band gaps (PBGs) in a photonic crystal (PC) to realize optical filters has attracted much attention in the optical and photonic communities. There are several ways of achieving PC-based optical filters. The simplest way is to introduce certain defect layer to break the translational symmetry in a periodic PC. With this defect, a transmission peak can be produced within the PBG and consequently the defective PC can work as a narrowband transmission filter or simply a multilayer Fabry-Perot resonator [1]. Filters with multiple channels within the PBG are of technical use and can be obtained by using another PC as a defect in the original host PC. This kind of defect is known as the photonic quantum well (PQW) structure and the appearance of multiple transmission peaks is ascribed to the photonic confinement [2,3]. If more channels are further needed, structures containing double-PQW or heterostructure-PC are available [4].

Another method of obtaining multichannel filter is to make use of the evanescent wave coupling in a defect-free PC. Such a kind of filter design is achieved by engineering the photonic pass bands. PCs containing metal, superconductor, single-negative (SNG) materials can be used to design such filters [5,6]. The common feature is that the permittivity must be negative in operating frequency region for these materials in order to possess the evanescent wave in. An all-dielectric PC can also be possible for this filter design based on the generation of

evanescent wave in the oblique incidence when the angle of incidence is greater than the critical angle for the interface from high-index medium to low-index medium [7,8].

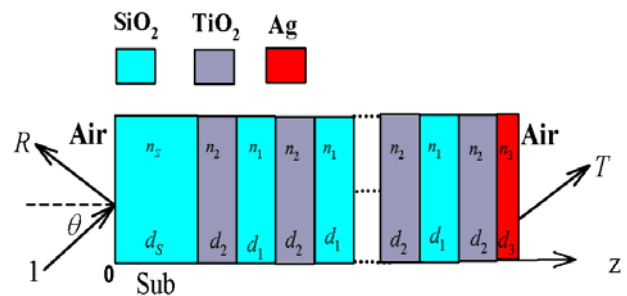


Fig. 1 The structure of the finite DDPC with a metal film at the rear side. It is denoted as Air/S(2/1)^N2/3/Air. Here, media 2 and 1 are TiO₂ and SiO₂, respectively, and the substrate S is also taken to be SiO₂. The layer 3 is the thin metallic film.

In addition to the above-mentioned methods, another filter design is to use composite structure made of dielectric-dielectric photonic crystal (DDPC) as well as thin metal film. Using ultrathin metal layer deposited on DDPC, a narrowband transmission-and-reflection filter can be achieved [9-11]. Such a filter possesses the simultaneous peaks at a certain wavelength in both the transmission and reflection spectra. A similar structure is shown in Fig. 1, in which a DDPC is coated with a thin metallic film at the rear side of the DDPC [12]. Unlike the

usual defective PC, this structure, which has no defect layer in the DDPC, can also possess the transmission peak inside the PBG of the original DDPC. In this case, the phenomenon of the presence of maximum transmission is referred to as the resonant optical transmission (ROT).

The purpose of this paper is to extend the study of Ref. [12] and to give a detailed analysis on the optical properties of ROT for the structure in Fig. 1. First, we shall investigate the phenomenon of ROT which can be present inside the PBG of the DDPC. To obtain a salient ROT, it will be found that there exist the optimum values in the number of periods and in the thickness of thin metal layer. We next explain mechanism of ROT by making use of the concept of impedance matching. Next, using different metal layers with different plasma frequency, it will be found the ROT can be affected by the metal chosen. Finally, we study the properties of ROT in the oblique incidence case for both the TE and TM waves. It will be seen that the frequency of ROT can be shifted as a function of the angle of incident, making the structure tunable and thus useful in the photonic applications.

2. Basic equations

The structure, Air/S(2/1)^N2/3/Air, considered in this work is depicted in Fig. 1. Here, media 2 and 1 are TiO₂ and SiO₂, respectively, and substrate S is also the same as SiO₂. Layer 3 is a thin metallic film. The incident wave with a unit power impinges at the left plane boundary with an angle of incidence θ_i . The reflectance and transmittance are denoted as R and T , respectively. To analyze the ROT, we adopt the transfer matrix method (TMM) to calculate R and T for the structure [13]. Following the TMM, we have the total transfer matrix for the system, i.e.,

$$\mathbf{M}_{\text{system}} = \begin{pmatrix} m_{11} & m_{12} \\ m_{21} & m_{22} \end{pmatrix} = \mathbf{D}_0^{-1} \mathbf{M}_{\text{Sub}} (\mathbf{M}_{\text{TiO}_2} \mathbf{M}_{\text{SiO}_2})^N \mathbf{M}_{\text{TiO}_2} \mathbf{M}_{\text{Ag}} \mathbf{D}_0, \quad (1)$$

where the transfer matrix in each layer is

$$\mathbf{M}_i = \mathbf{D}_i \mathbf{P}_i \mathbf{D}_i^{-1}, \quad i = 1 \text{ (SiO}_2\text{)}, 2 \text{ (TiO}_2\text{)}, 3 \text{ (Ag)} \quad (2)$$

where the propagation matrix in layer i is expressed as

$$\mathbf{P}_i = \begin{pmatrix} \exp(jk_i d_i) & 0 \\ 0 & \exp(-jk_i d_i) \end{pmatrix}, \quad (3)$$

where $k_i = (\omega/c)n_i \cos \theta_i = (\omega/c)\sqrt{\epsilon_i} \cos \theta_i$

and d_i are the wave number and thickness in layer i , respectively. The dynamical matrix in medium i is written by

$$\mathbf{D}_i = \begin{pmatrix} 1 & 1 \\ n_i \cos \theta_i & -n_i \cos \theta_i \end{pmatrix}, \quad (4)$$

for TE wave and

$$\mathbf{D}_i = \begin{pmatrix} \cos \theta_i & \cos \theta_i \\ n_i & -n_i \end{pmatrix}, \quad (5)$$

for TM wave, respectively. The transmittance T and reflectance R for the multilayer structure in Figure 1 can be determined by the following equations,

$$T = |t|^2 = \left| \frac{1}{m_{11}} \right|^2, \quad R = |r|^2 = \left| \frac{m_{21}}{m_{11}} \right|^2. \quad (6)$$

3. Numerical results and discussion

Let us first investigate the photonic band gap for an ideal DDPC without a metallic coating, i.e., the structure is Air/S(2/1)^N2/Air. With the material parameters, $n_1 = 1.46$ (SiO₂), $n_2 = 2.25$ (TiO₂), $d_1 = 102.7$, $d_2 = 65.3$ nm, and $N = 20$ [12]. In addition, the most left substrate is taken as SiO₂ with a thickness of 400 nm. In Fig. 2, we have plotted R (blue) and T (red) spectra for the case of normal incidence. It can be seen that there exists a PBG (the stop band) in the visible and it has the lower and upper band edges at $f_L = 4.37 \times 10^{14}$ Hz (686.5 nm) and $f_H = 5.74 \times 10^{14}$ Hz (522.6 nm), respectively.

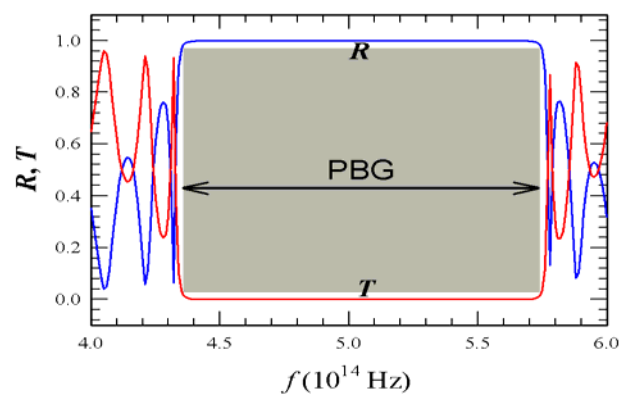


Fig. 2 Calculated R (blue curve) and T (red curve) spectra for the structure without a metallic coating, i.e., Air/S(2/1)^N2/Air. A PBG exists in the visible and ranges from 4.37×10^{14} to 5.74×10^{14} Hz.

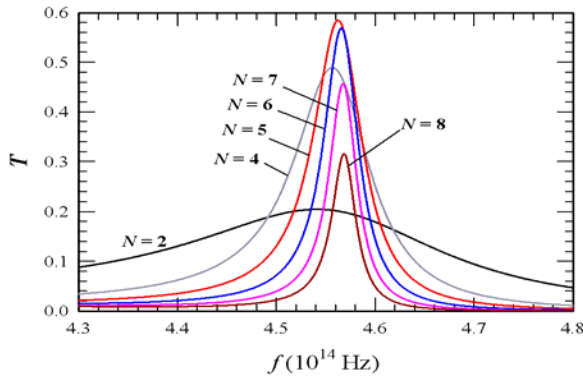


Fig. 3 Calculated transmittance spectra for the structure with a metallic coating, $\text{Air}/\text{S}(2/1)^N 2/3/\text{Air}$, at different numbers of stack numbers, $N = 2, 4, 5, 6, 7,$ and 8 , respectively. The ROT with a peak height larger than 0.5 can be seen for $N = 5$ and 6 .

Now with a metallic coating of Ag at the rear side as shown in Fig. 1, $\text{Air}/\text{S}(2/1)^N 2/3/\text{Air}$. Here, the permittivity of Ag is described by the Drude model, namely [14]

$$\epsilon_3(\omega) = 1 - \frac{\omega_p^2}{\omega^2 - j\gamma\omega}, \quad (7)$$

where ω_p and γ are the plasma and damping frequencies, respectively. With film thickness $d_3 = 40$ nm and $\omega_p = 1.37 \times 10^{16}$, $\gamma = 7.29 \times 10^{13}$ rad/s [12], the calculated transmittance is shown in Fig. 3. It can be seen there is a ROT within the PBG in Fig. 2 and it strongly depends on the stack number N . There exists certain optimum number in N . The peak height of ROT can be larger than 0.5 when $N = 5$ and 6 . Thus, $N = 5$ can be the optimum condition for obtaining the maximum ROT. In this case, the frequency of ROT is found to be 4.56×10^{14} Hz and peak height is 0.585.

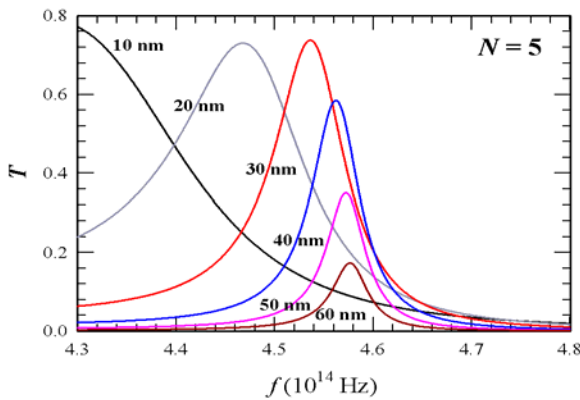


Fig. 4. Calculated transmittance spectra for the structure with a metallic coating, $\text{Air}/\text{S}(2/1)^N 2/3/\text{Air}$, at different thicknesses of Ag, $d_3 = 10, 20, 30, 40, 50,$ and 60 nm, respectively, for a fixed stack number of $N = 5$. The ROT with a maximum peak height of 0.737 at 4.537×10^{14} Hz can be obtained for $d_3 = 30$ nm.

Fig. 4 shows the transmittance at $N = 5$ for distinct thicknesses of Ag, $d_3 = 10, 20, 30, 40, 50,$ and 60 nm, respectively. The phenomenon of ROT is strongly dependent on the thickness of Ag. It can be seen from the figure that, at 30 nm, the transmittance attains the maximum value of 0.737. For thickness larger than 30 nm, the peak height decreases fast as the thickness increases. Conclusively, there is also an optimum thickness of Ag in order to have a salient ROT within the PBG.

The phenomenon of ROT shown in Figs. 3 and 4 can be explained by the concept of impedance matching. The normalized effective surface impedance $z_{s,eff}$ at the plane boundary $z = 0$ can be calculated through the reflection coefficient r , namely [1]

$$z_{s,eff} = r_{s,eff} + jx_{s,eff} \equiv \frac{Z_{s,eff}}{Z_0} = \frac{1+r}{1-r}, \quad (8)$$

where r is calculated by Eq. (6), $Z_{s,eff} = R_{s,eff} + jX_{s,eff}$ is the effective surface impedance at $z = 0$, and $Z_0 = 377 \Omega$ is the intrinsic impedance of air. For a simple lossless system, the resonant transmission occurs at frequency of zero reflection, $r = 0$, which in turn leads to a maximum surface resistance and zero surface reactance, $r_{s,eff} = 1$ and $x_{s,eff} = 0$. In the $r_{s,eff}$ - and $x_{s,eff}$ -plot, this corresponds to the resonant point. At the resonant point, the entire structure reaches the impedance match, matching to the impedance of air impedance. Fig. 5 shows the calculated T , $r_{s,eff}$, and $x_{s,eff}$ in the vicinity of ROT. Taking a look at $r_{s,eff}$ - and $x_{s,eff}$ -plot reveals that the resonant point, where $r_{s,eff}$ attains a maximum and $x_{s,eff}$ is at the turning point, is very close to ROT. That is, the ROT phenomenon can be approximately explained by the concept of impedance match.

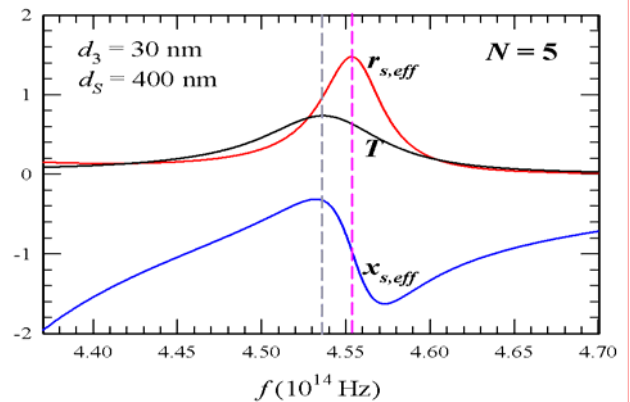


Fig. 5 Calculated transmittance T , normalized effective surface resistance $r_{s,eff}$, and normalized surface reactance $x_{s,eff}$ at $N = 5, d_3 = 30$ nm and $d_s = 400$ nm.

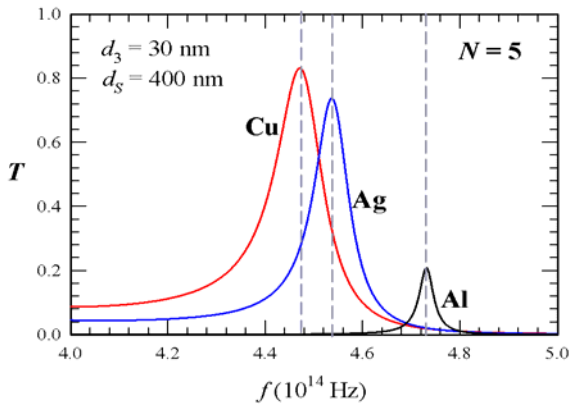


Fig. 6 Calculated transmittance T at $N = 5$, and $d_3 = 30$ nm for metal films of Cu, Ag, and Al, respectively.

We now examine how the ROT is influenced by using different metals. Here, Cu, Ag and Al will be used for the purpose of comparison. With the same thicknesses for dielectric layers and $N = 5$, $d_3 = 30$ nm, in Fig. 6, we plot the transmittance for metal films of Cu, Ag, and Al, respectively. Here, the plasma and damping frequencies are: Cu, $\omega_p = 1.20 \times 10^{16}$, $\gamma = 5.18 \times 10^{13}$ rad/s, and Al, $\omega_p = 2.24 \times 10^{16}$, $\gamma = 12.19 \times 10^{13}$ rad/s [15]. The results show that Cu, which has the lowest value in plasma frequency, has a maximum peak height of ROT and its peak frequency is also red-shifted compared to Ag. For Al with a higher plasma frequency than Ag will thus blue-shifted. In addition, its strength of ROT is significantly lowered down because of its strong damping frequency.

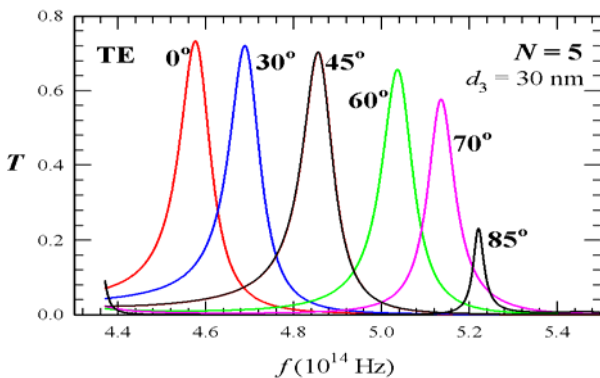


Fig. 7 Calculated transmittance T at $N = 5$, $d_s = 400$ nm, and $d_3 = 30$ nm for different angles of incidence, $\theta = 0^\circ$, 30° , 45° , 60° , 70° , and 85° , respectively, under the TE wave.

We have investigated the properties of ROT in the normal incidence. Let us extend the study to the case of oblique incidence. With the same thicknesses for dielectric layers and $N = 5$, $d_s = 400$ nm, $d_3 = 30$ nm for Ag, in Figure 7, we plot the TE-wave transmittance for various angles of incidence, $\theta = 0^\circ$, 30° , 45° , 60° , 70° , and 85° , respectively. It is seen that the frequency of ROT is

blue-shifted as the angle increases. In addition, the peak height of ROT is strongly reduced at a large angle of incident. For instance, the peak height is about 0.225 at 85° .

Fig. 8 depicts the TM-wave transmittance for various angles of incidence, $\theta = 0^\circ$, 30° , 45° , 60° , and 70° , respectively. Like in the TE-wave, the frequency of ROT is again blue-shifted as the angle of incidence increases. The peak height is now gradually enhanced as a function of angle, which is in contrast to the case of TE wave. Finally, it is of interest to note that a second ROT near 4.7×10^{14} Hz is found at a large angle of 70° . In fact, for angles larger than 70° , such double peaks are seen and their behaviors are illustrated in Fig. 9. Some features are of note. First, at a fixed angle of incidence, the peak height at lower frequency is lower than that of higher frequency. Second, the two frequencies of ROT are blue-shifted as the angle increases. Third, the peak of lower frequency of ROT increases and the shape is narrowed as the angle increase. However, the peak height of higher frequency of ROT slightly increases until 80° and then decreases when the angle increases. At angle near glancing incidence, the two peaks become very sharp and their heights are comparable.

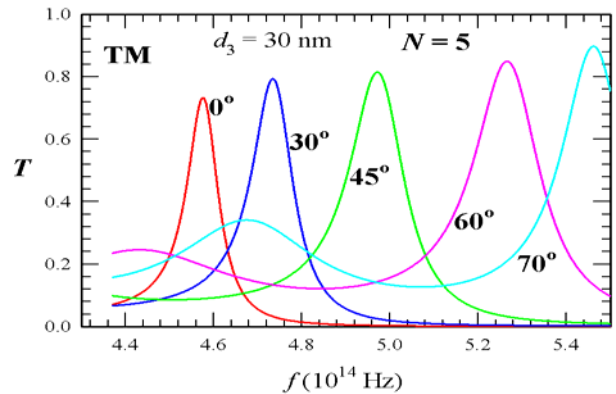


Fig. 8 Calculated transmittance T at $N = 5$, $d_s = 400$ nm, and $d_3 = 30$ nm for different angles of incidence, $\theta = 0^\circ$, 30° , 45° , 60° , and 70° , respectively, under the TM wave.

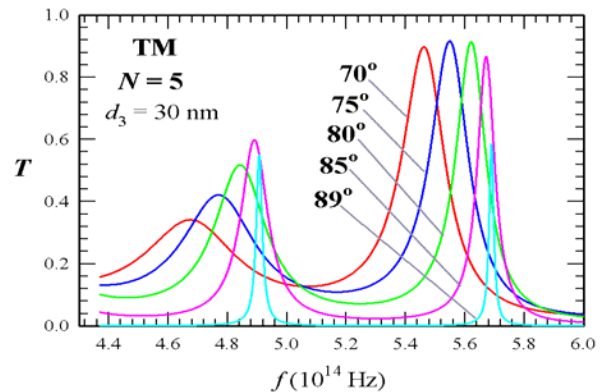


Fig. 9 Calculated TM-wave transmittance T at $N = 5$, $d_s = 400$ nm, and $d_3 = 30$ nm for the large angles of incidence, $\theta = 70^\circ$, 75° , 80° , 85° , and 89° , respectively.

Before we go into the conclusion, we mention that the ROT can also be seen when we place the metal film in the front side of DDPC instead of in the rear side in Fig. 1. In this case, the structure is $\text{Air}/3(2/1)^N/\text{Air}$, where the substrate is removed. With the same material parameters in Fig. 7, In Fig. 10, we show the calculated TE-wave transmittance for various angles of incidence, $\theta = 0^\circ, 30^\circ, 45^\circ, 60^\circ, 70^\circ$, and 85° , respectively. It can be seen that the ROT remains available. Like in Fig. 7, the frequency of ROT is also blue-shifted as the angle increases. In addition, its peak height decreases monotonously as a function of the angle of incidence. The decreasing trend is more pronounced compared to Fig. 7. Another feature of note is that, at 85° , two ROT peaks are seen at frequencies of 4.43×10^{14} and 5.23×10^{14} Hz. The result of double peaks has been seen in Fig. 9, which is for the metal in the rear side of DDPC. However, the peak heights of these two ROTs are relatively small. As for the TM wave, the ROT curves (not shown) are very similar to those in Fig. 8, excepting that the low-frequency ROT at 70° in Fig. 9 does not appear.

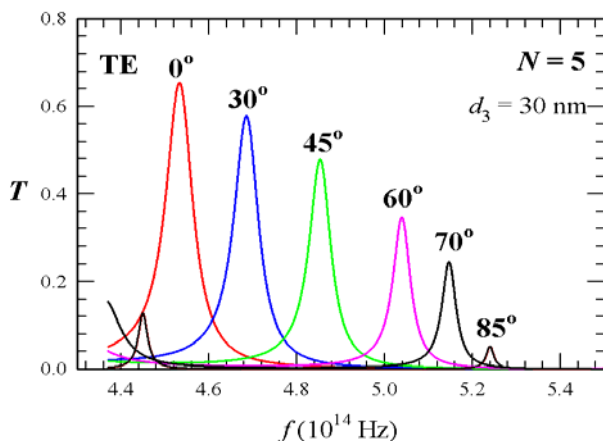


Fig. 10 Calculated transmittance T at $N = 5$ and $d_3 = 30$ nm (Ag) for different angles of incidence, $\theta = 0^\circ, 30^\circ, 45^\circ, 60^\circ, 70^\circ$, and 85° , respectively, under the TE wave.

4. Conclusion

The optical properties of ROT for a $\text{SiO}_2\text{-TiO}_2$ photonic crystal with a thin metal coating have been theoretically analyzed. Two possible configurations, DDPC-M and M-DDPC, have been studied. With the inclusion of thin metal layer, it is shown that the ROT can be found with the photonic band gap for these two configurations. To obtain the ROT, we find that there exist an optimum number of periods in the DDPC and an optimum thickness of the metal film. We have successfully explained the phenomenon of ROT by using the impedance matching concept. In the oblique case, the frequency of ROT is found to be blue-shifted as a function of angle of incidence for both TE and TM waves. This feature suggests that the angle of incidence can play as a tuning agent that makes the structure tunable. In the TM

wave, there are two ROTs at larger angles of incidence. The existence of double peaks can increase the spectral efficiency of bandwidth utilization when engineering the PBG to realize the filter based on the use of the DDPC.

Acknowledgment

C.-J. Wu acknowledges the financial support from the National Science Council of the Republic of China (Taiwan) under Contract No. NSC-100-2112-M-003-005-MY3.

References

- [1] S. J. Orfanidis, *Electromagnetic Waves and Antennas*, Rutgers University, www.ece.rutgers.edu/~orfanidi/ewa (2010).
- [2] F. Qiao, C. Zhang, and J. Wan, *Appl. Phys. Lett.* **77**, 3698 (2000).
- [3] Y.-H. Chang, Y.-Y. Jhu, and C.-J. Wu, *J. Optoelectron. Adv. Mater.* **14**, 185 (2012).
- [4] H.-C. Hung, C.-J. Wu, and S.-J. Chang, *IEEE J. Quan. Electron.* **48**, 361 (2012).
- [5] W.-H. Lin, C.-J. Wu, T.-J. Yang, and S.-J. Chang, *Opt. Exp.* **18**, 27155 (2010).
- [6] S. Feng, J. M. Elson, and P. L. Overfelt, *Opt. Exp.* **13**, 4113 (2005).
- [7] Y.-T. Fang, Z.-C. Liang, *Opt. Commun.* **283**, 2102 (2010).
- [8] L. Jin, J. Zhou, C. Xue, M. He, S. Huang, *Optik* **123**, 1030 (2012).
- [9] W. Shen, X. Sun, Y. Zhang, Z. Luo, X. Liu, P. Gu, *Opt. Commun.* **282**, 242 (2009).
- [10] Y.-H. Chang, C.-C. Liu, T.-J. Yang, and C.-J. Wu, *J. Opt. Soc. Am. B* **26**, 1141 (2009).
- [11] C.-C. Liu, Y.-H. Chang, T.-J. Yang, C.-J. Wu, *Prog. Electromagn. Res.* **96**, 329 (2009).
- [12] C.-S. Yuan, H. Tang, C. He, X.-L. Chen, X. Ni, M.-H. Lu, Y.-F. Chen, N.-B. Ming, *Physica B* **406**, 1983 (2011).
- [13] P. Yeh, *Optical Waves in Layered Media*, John Wiley & Sons, Singapore (1991).
- [14] C. Sabah, S. Uckun, *Prog. Electromagn. Res.* **91**, 349 (2009).
- [15] C.-J. Wu, H.-C. Lin, *Opt. Rev.* **18**, 338 (2011).

*Corresponding author: jasperwu@ntnu.edu.tw